Reduction rates of MnO and SiO_2 in SiMn slags between 1500 and 1650°C

P.P. Kim[1], T.A. Larssen[1], and M. Tangstad[1]

Affiliation:
1 Department of Materials Science and Engineering, Norwegian University of Science and Technology, N-7591 Trondheim, Norway.

Correspondence to:
P.P. Kim

Email:
pyung.h.kim@ntnu.no

Dates:
Received: 30 Mar. 2018
Revised: 2 Oct. 2018
Accepted: 29 Oct. 2018
Published: May 2019

How to cite:
Kim, P.P., Larssen, T.A., and Tangstad, M.
Reduction rates of MnO and SiO_2 in SiMn slags between 1500 and 1650O°C
The Southern African Insitute of Mining and Metallurgy

DOI ID:
http://dx.doi.org/10.17159/2411-9717/153/2019

ORCiD ID:
P.P. Kim
https://orchid.org/0000-0001-5449-5385
T.A. Larssen
https://orchid.org/0000-0003-0224-3201
M. Tangstad
https://orchid.org/0000-0001-9751-7716

Synopsis

The kinetics of MnO and SiO_2 reduction in SiMn slags based on Assmang/Comilog ore and HCFeMn (high-carbon ferromanganese) slag were investigated between 1500 and 1650°C under a CO atmosphere. The results showed that charges containing HCFeMn slag had relatively faster reduction rates than those without. The difference in the driving force for MnO reduction was insignificant among the SiMn slags at 1500°C, which implies a low contribution of the driving force for reduction rate. The slag viscosities were also rather similar, around 1 poise at 1500°C, which could not explain the different reduction rates. Instead, the different charges containing various sulphur contents are believed to give rise to the varying reduction rates. The estimated activation energies for MnO reduction were around 500–920 kJ/mol for charges containing HCFeMn slag, and between 250–300 kJ/mol for those without. Based on the estimated kinetic parameters, the considered rate models were able to describe the reduction of MnO and SiO_2 in SiMn slags between 1500 and 1650°C.

Keywords
SiMn, MnO, SiO_2, reduction, kinetics.

Introduction

Manganese ferroalloys such as ferromanganese (FeMn) and silicomanganese (SiMn) are important ingredients in steel production due to the beneficial effects of manganese on the physical properties of steel. Mn enhances the strength, toughness, and hardness of steel products, and both Mn and Si are used as deoxidizers to prevent the development of porous structures (International Manganese Institute, 2014; Olsen, Tangstad, and Lindstad, 2007; Subramanyam, Swansiger, and Avery, 1990; Tomota *et al.,* 1987).

The thermodynamic background of manganese ferroalloys is well established (Olsen, Tangstad and Lindstad, 2007), but kinetic information is rather scarce, especially for the SiMn process (Tranell *et al.,* 2007; Tore-Andre Skjervheim, 1994). The absence of kinetic information makes it more difficult to understand the reduction mechanisms of MnO and SiO_2. It is not clear how different raw materials affect the SiMn process. The main metal-producing reactions in the SiMn process are described by Equations [1] and [2]:

$$MnO_{(l)} + C \rightarrow Mn_{(l)} + CO_{(g)} \quad [1]$$

$$SiO_{2(l)} + 2C \rightarrow Si_{(l)} + 2CO_{(g)} \quad [2]$$

Recent studies have shown that MnO and SiO_2 are reduced to Mn and Si significantly above 1500°C (Kim, Holtan, and Tangstad, 2016; Kim *et al.,* 2017). The mass change observed in thermogravimetric experiments was low until 1500°C, but increased significantly at higher temperatures. It was perceived that most of the MnO and SiO_2 reduction occurred between 1500 and 1650°C, but the reasons were not fully understood. Therefore, the present study focuses on the kinetic information on MnO and SiO_2 reduction in SiMn slags ($MnO-SiO_2-CaO-MgO-Al_2O_3$) between 1500 and 1650°C using different Mn sources.

Theoretical considerations

The reduction rate of MnO was studied previously and was described by Equation [1] (Olsen, Tangstad, and Lindstad, 2007; Ostrovski *et al.,* 2002). This equation is based on the FeMn process and implies that the chemical reaction is the rate-determining step. Since SiMn slags are essentially similar to FeMn slags, Equation [1] can also be used for MnO reduction from SiMn slags. For SiO_2, a recent study showed that the dissolution of SiO_2 into slag was the rate-determining step (Maroufi *et al.,* 2015). However, contrary results have also been observed where the dissolution of both MnO and SiO_2 into slag was completed before significant reduction takes place above 1500°C (Kim and Tangstad, 2018a, 2018b, 2018c; Holtan, 2015). In this study, a similar rate equation for SiO_2 reduction was presumed using Equation [2], assuming SiO_2 reduction is also mainly controlled by chemical reaction. Both Equations [1] and [2] were considered in this work to estimate the kinetic parameters.

For Equation [1]:

$$r_{MnO} = k_{MnO} \cdot A \cdot (a_{MnO} - a_{MnO,Eqm.}) = k_{o,MnO} \cdot A \cdot e^{-E_{MnO}/RT} \cdot (a_{MnO} - \frac{a_{Mn}}{K_{T,MnO}})$$

For Equation [2]:

$$r_{SiO_2} = k_{SiO_2} \cdot A \cdot (a_{SiO_2} - a_{SiO_2,Eqm.}) = k_{o,SiO_2} \cdot A \cdot e^{-E_{SiO_2}/RT} \cdot (a_{SiO_2} - \frac{a_{Si}}{K_{T,SiO_2}})$$

where r is the reduction rate (g/min), k is the rate constant (g/min·cm^2), k_o is the frequency factor, A is the reaction area (cm^2), E is the activation energy (kJ/mol), R is the gas constant, T is the temperature, a_{MnO}, a_{SiO_2} are the activity values of MnO and SiO_2 in the slag phase, $a_{MnO,Eqm.}$, $a_{SiO_2,Eqm.}$ are the activity values of MnO and SiO_2 in equilibrium, and K_T is the equilibrium constant at temperature T.

The rate models considered for MnO and SiO_2 reduction also imply that the driving force, which is the difference between the activity of slag (MnO, SiO_2) and the produced metal (Mn, Si), contribute to the reduction rates. The simplified models for activities of slag and metal have been recently studied (Olsen, 2016). These activities were based on FactSage 7.0, database FTOxid and FactPS (CRCT and GTT, 2015), and thermodynamic data from HSC Chemistry 7 (Outotec, n.d.) was used to calculate the driving forces of MnO and SiO_2 reduction at different temperatures.

Experimental procedures

The chemical compositions of the raw materials are shown in Table I and the SiMn charges are described in Table II. Note that manganese is present as MnO and MnO_2 in manganese ores. Three different Mn sources, Assmang ore, Comilog ore, and HCFeMn slag, were used to study different SiMn charges in this work. The sizes of the raw materials were between 0.6 and 1.6 mm. Each raw material was weighed to aim at approximately 40 wt% SiO_2 in slag and 18 wt% Si in the metal phase, which is close to the thermodynamic equilibrium at 1600°C (Olsen, Tangstad, and Lindstad, 2007). The charge materials were added into graphite crucibles (36 mm outer diameter, 30 mm inner diameter, 70 mm height, and 61 mm depth).

A TGA furnace, which is schematically depicted in Figure 1, was used to conduct the experiments. The furnace can reach temperatures up to 1700°C and the maximum heating rate is 25°C/min. A mass balance is installed at the top and a molybdenum (Mo) wire was used to suspend the graphite crucible inside the chamber. The temperature schedule of the experiment was considered to simulate an industrial furnace operation and is described in Figure 2. Initially, the furnace was rapidly heated up

Table I

Chemical composition of raw materials (wt%)

Material	MnO	MnO_2	SiO_2	Fe_2O_3	CaO	MgO	Al_2O_3	S	C	CO_2	H_2O	Total
Assmang	32.7	33.2	5.8	15.1	6.3	1.1	0.3	0.16	0.3	3.5	1.6	100.6
Comilog	3.0	72.4	4.6	6.7	0.1	0.1	5.6	-	-	0.1	5.0	97.6
Quartz	0.1	-	93.9	-	0.1	0.1	1.2	-	-	-	-	95.4
HCS*	35.2	-	25.5	-	18.5	7.5	12.3	0.46	0.4	-	2.2	102.1
Coke	-	-	5.6	0.86	0.4	0.2	2.8	0.4	87.7	-	15.5	113.5

* HCS: high-carbon FeMn slag

Table II

Composition of SiMn charges used in the experiments (g)

Charge	Assmang*	Comilog*	Quartz	HCS*	Coke	Total
As	7	-	1.9	-	2.2	11.1
As/HCS	4	-	1.7	4	2.5	12.2
Com	-	6	1.4	-	2.0	9.4
Com/HCS	-	4	1.6	4	2.3	11.9
HCS	-	-	1.5	10	3.0	14.5

* Mn-bearing materials

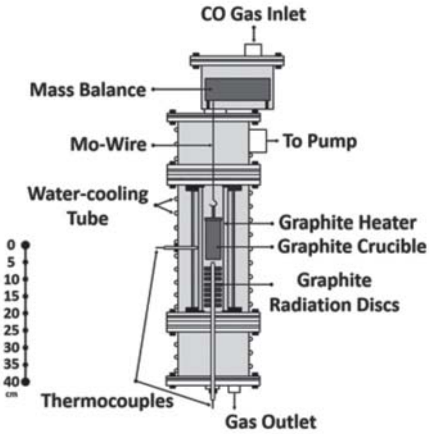

Figure 1—Schematic of the TGA furnace

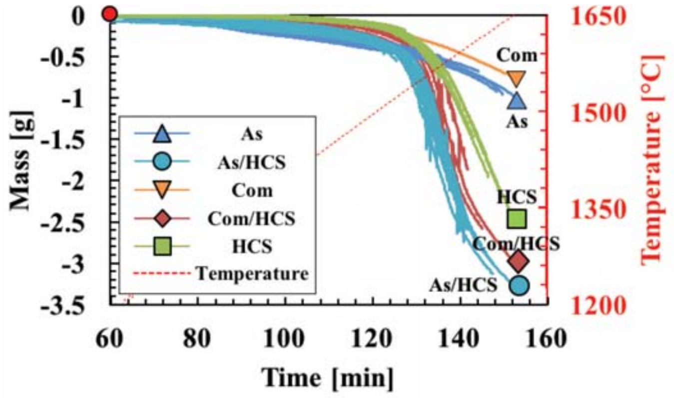

Figure 3 – TGA results for several experiments for each charge between 1500 and 1650°C, with respect to the new reference point (red circle) at 1200°C

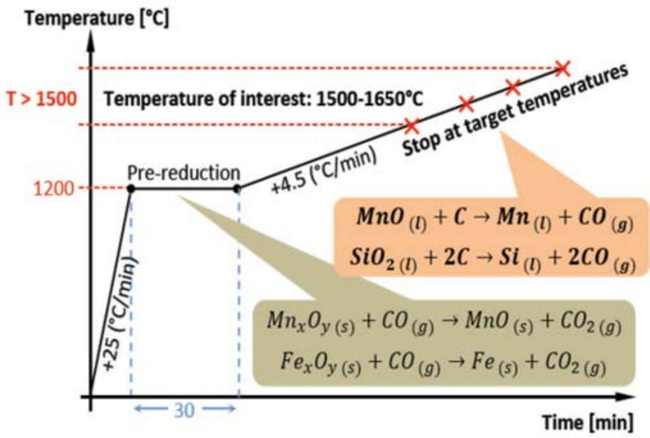

Figure 2—The temperature schedule

to 1200°C at a rate of 25°C/min and held for 30 minutes to secure complete prereduction (Olsen, Tangstad, and Lindstad, 2007). Then, further heating at a rate of 4.5°C/min was done and stopped at targeted temperatures between 1500 and 1650°C, followed by cooling. All experiments were conducted in CO at atmospheric pressure.

The weight loss of each charge sample was recorded and the data was logged every 5 seconds during the experiment. Lastly, a portion from each charge sample was prepared by mounting it in epoxy for electron probe microanalysis (EPMA) using a JEOL JXA-8500F instrument. The average slag composition from more than five analysed points was used to calculate the metal composition (as the metal analyses are more uncertain than the slag analyses).

Results and discussion

The mass changes recorded during the TGA runs were the main information used. Figure 3 describes the TGA results from different SiMn charges between 1200 and 1650°C. Note that complete prereduction was assumed at 1200°C and used as a new reference point for further reduction of MnO and SiO_2. The mass changes for all SiMn charges were insignificant below 1500°C, which indicated a low degree of MnO and SiO_2 reduction. The reduction rate increased above 1500°C, which is in accordance with previous studies (Kim, Holtan, and Tangstad, 2016; Kim *et al.,* 2017), but the degree of reduction differed with different SiMn charges. It was observed that charges containing HCFeMn slag were reduced faster and attained higher degrees of reduction. Although the apparent accelerated reduction can be thought to result from the use of HCFeMn slag, the TGA results

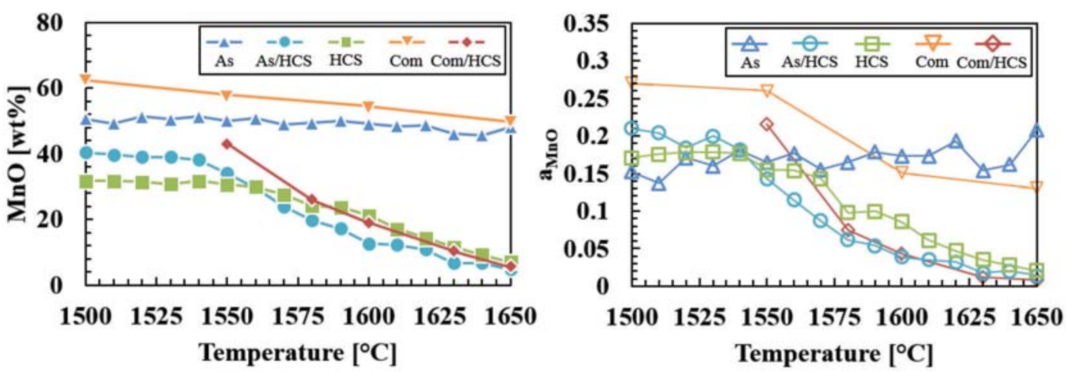

Figure 4 – Comparison of MnO (left) and a_{MnO} (right) between 1500 and 1650°C

Table III

Slag analyses (EPMA) and calculated metal compositions with the respective activities between 1500 and 1650°C

Charge temp.	Slag (wt%)								Metal (calculated, wt%)					
	MnO	SiO_2	CaO	MgO	Al_2O_3	a_{MnO}	$aSiO_2$	C+M/A	Mn	Si	Fe	C	a_{Mn}/KT	a_{Si}/KT
As-1500	50.6	39.1	7.6	1.2	0.5	0.152	0.285	17.2	54.6	4.3	35.9	5.2	0.0037	0.1280
1510	49.3	40.5	7.7	1.3	0.7	0.137	0.339	13.7	55.9	2.0	35.9	6.2	0.0035	0.0378
1520	51.3	37.9	7.2	1.3	0.5	0.171	0.237	16.0	54.4	7.4	34.0	4.2	0.0030	0.1914
1530	50.5	38.8	7.7	1.2	0.5	0.160	0.269	16.4	55.2	5.8	34.3	4.6	0.0029	0.0994
1540	51.4	37.4	8.4	0.7	0.7	0.181	0.218	13.3	55.0	8.8	32.6	3.5	0.0026	0.1598
1550	50.1	38.7	8.3	0.8	0.7	0.165	0.258	12.7	56.4	7.4	32.2	4.1	0.0025	0.0915
1560	50.8	37.9	7.5	1.4	0.5	0.177	0.229	16.3	55.8	8.7	31.7	3.8	0.0021	0.1026
1570	49.0	39.7	7.7	1.3	0.5	0.155	0.289	16.6	57.6	6.7	31.3	4.5	0.0021	0.0504
1580	49.4	39.0	8.6	0.7	0.8	0.165	0.261	11.7	57.5	8.1	30.6	3.9	0.0019	0.0543
1590	50.1	38.2	8.9	0.8	0.7	0.179	0.230	13.4	57.1	9.4	30.1	3.4	0.0017	0.0587
1600	49.1	38.7	8.9	0.7	0.9	0.173	0.243	11.1	58.3	9.7	28.6	3.5	0.0016	0.0511
1610	48.4	38.8	9.1	0.7	0.8	0.173	0.240	12.5	59.1	10.4	27.3	3.2	0.0015	0.0479
1620	48.7	37.7	9.4	0.7	0.9	0.193	0.198	11.0	59.2	12.3	25.8	2.7	0.0013	0.0581
1630	46.1	40.5	8.0	1.4	0.8	0.154	0.289	11.6	60.8	9.9	25.6	3.6	0.0013	0.0311
1640	45.7	40.1	9.3	1.4	0.8	0.162	0.263	13.3	61.1	11.3	24.3	3.3	0.0011	0.0339
1650	48.1	37.3	7.5	1.3	0.7	0.208	0.175	12.0	59.6	13.5	24.2	2.8	0.0009	0.0443
As/HCS-1500	40.5	35.1	12.3	3.8	5.2	0.210	0.107	3.1	50.0	10.7	36.5	2.9	0.0031	
1510	39.8	35.4	12.2	3.5	5.8	0.204	0.111	2.7	52.7	10.6	33.8	3.0	0.0030	0.4818
1520	39.1	36.6	12.0	3.9	5.6	0.184	0.135	2.9	54.5	5.2	35.6	4.7	0.0032	0.1010
1530	39.1	35.7	12.1	3.7	4.9	0.200	0.113	3.3	54.6	10.5	31.8	3.1	0.0026	0.2934
1540	38.3	36.8	12.2	3.9	5.0	0.182	0.135	3.2	56.8	6.4	32.4	4.4	0.0028	0.0904
1550	34.1	39.0	13.2	3.7	6.3	0.143	0.168	2.7	64.8	6.5	24.1	4.6	0.0029	0.0734
1560	29.5	40.4	14.4	4.0	6.7	0.115	0.182	2.7	68.4	8.9	18.7	3.9	0.0027	0.1021
1570	24.0	41.8	16.2	4.3	8.0	0.087	0.187	2.6	70.2	11.1	15.3	3.4	0.0024	0.1244
1580	19.7	44.1	18.3	5.2	8.8	0.062	0.227	2.7	72.0	10.3	14.1	3.7	0.0023	0.0838
1590	17.2	44.2	19.2	5.2	9.2	0.054	0.212	2.7	71.8	11.6	13.2	3.4	0.0020	0.0882
1600	12.7	43.8	21.6	6.2	10.4	0.039	0.174	2.7	71.3	13.9	12.0	2.9	0.0016	0.1094
1610	12.3	45.4	21.2	6.0	10.7	0.035	0.213	2.6	72.2	12.4	12.1	3.2	0.0016	0.0682
1620	10.9	44.6	22.5	6.4	11.5	0.032	0.183	2.5	71.6	13.7	11.7	3.0	0.0014	0.0710
1630	6.8	45.5	24.2	6.7	12.4	0.018	0.181	2.5	71.8	14.1	11.1	2.9	0.0013	0.0637
1640	6.8	44.0	24.9	7.2	12.8	0.020	0.147	2.5	71.0	15.2	11.0	2.8	0.0011	0.0651
1650	4.9	43.9	26.5	7.1	13.8	0.014	0.136	2.4	70.9	15.7	10.7	2.8	0.0010	0.0591
HCS-1500	31.7	34.5	15.4	4.9	9.4	0.171	0.076	2.2	27.3	30.1	36.2	6.4	0.0005	-
1510	31.7	34.2	15.8	5.0	9.7	0.176	0.072	2.2	29.7	32.4	27.2	10.7	0.0002	-
1520	31.5	34.1	15.9	5.1	9.7	0.178	0.069	2.2	35.5	32.1	22.2	10.2	0.0002	-
1530	30.8	33.8	15.8	5.2	10.0	0.179	0.064	2.1	43.8	31.5	15.0	9.6	0.0001	-
1540	31.7	34.4	15.8	5.5	9.2	0.177	0.074	2.3	28.6	30.7	33.2	7.6	0.0002	-
1550	30.6	35.8	16.1	5.6	9.5	0.155	0.092	2.3	58.6	0.1	34.5	6.9	0.0027	-
1560	30.0	35.7	16.3	5.8	9.7	0.154	0.090	2.3	63.9	8.8	23.5	3.9	0.0025	0.1012
1570	27.6	35.6	16.9	5.8	10.0	0.143	0.080	2.3	68.5	18.9	10.1	2.5	0.0013	0.5175
1580	24.1	38.8	17.3	5.5	11.3	0.098	0.124	2.0	82.1	3.4	8.2	6.3	0.0028	0.0126
1590	23.7	38.4	17.5	5.8	11.4	0.100	0.116	2.1	80.5	7.0	7.6	5.0	0.0025	0.0302
1600	21.2	38.8	18.5	6.2	11.5	0.086	0.114	2.2	79.9	10.4	5.9	3.9	0.0021	0.0507
1610	17.1	40.1	19.4	6.3	12.9	0.061	0.124	2.0	80.8	10.8	4.6	3.8	0.0019	0.0444
1620	14.3	40.8	21.3	6.8	13.3	0.047	0.127	2.1	80.8	11.6	4.0	3.7	0.0017	0.0423
1630	11.6	41.5	22.9	7.1	13.9	0.035	0.130	2.2	80.8	12.1	3.6	3.6	0.0016	0.0385
1640	9.2	40.2	23.6	7.8	15.3	0.028	0.097	2.0	77.7	16.4	3.2	2.9	0.0010	0.0694
1650	7.1	40.2	25.5	7.8	15.9	0.021	0.092	2.1	77.3	17.0	3.0	2.8	0.0009	0.0657
Com-1500	62.4	28.8	0.1	0.2	2.5	0.306	0.106	0.1	51.8	14.3	31.7	2.2	0.0028	1.2916
1550	57.9	30.4	0.3	0.2	4.4	0.264	0.136	0.1	66.3	15.0	16.2	2.5	0.0022	0.4250
1600	54.7	30.0	0.4	0.2	5.3	0.242	0.138	0.1	68.8	16.5	12.2	2.5	0.0013	0.1802
1650	49.7	35.5	0.3	0.2	5.6	0.161	0.261	0.1	71.8	12.9	12.1	3.2	0.0012	0.0359
Com/HCS-1550	43.1	33.9	9.0	3.6	7.4	0.220	0.113	1.7	61.7	9.8	25.0	3.5	0.0026	0.1588
1580	26.2	41.3	13.0	4.4	11.8	0.077	0.225	1.5	78.4	9.9	7.8	4.0	0.0025	0.0714
1600	19.0	43.0	14.7	5.1	14.2	0.045	0.234	1.4	78.3	11.9	6.4	3.5	0.0020	0.0694
1630	10.4	43.3	19.0	6.5	17.7	0.019	0.200	1.4	77.0	14.6	5.4	3.0	0.0013	0.0638
1650	5.7	40.9	22.2	7.6	20.6	0.009	0.134	1.5	75.1	17.1	5.0	2.8	0.0026	0.1588

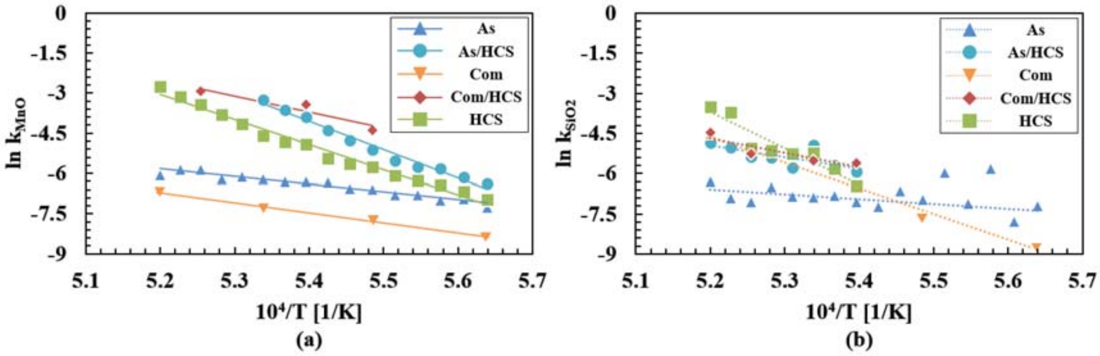

Figure 5—Arrhenius plots of (a) MnO reduction and (b) SiO_2 reduction between 1500 and 1650°C

do not adequately describes the reduction degrees of MnO and SiO_2 separately. Quantitative slag and metal analyses are required to provide further information.

The average slag and metal compositions of the different charges, with their respective activities (slag: a_{MnO} and a_{SiO_2}, metal: a_{Mn}/K_T and a_{Si}/K_T), between 1500 and 1650°C are shown in Table III. Significant reduction of MnO was clearly observed with charges containing HCFeMn slag. The MnO content in slag between 1500 and 1650°C for charges 'As/HCS' and 'HCS' decreased from approximately 40 and 31 wt% to 5 and 7 wt%, respectively. Similar degrees of reduction were also observed from charge 'Com/HCS', where the decrease of MnO was from approximately 43 to 6 wt% between 1500 and 1650°C. On the other hand, for charges without HCFeMn slag ('As' and 'Com') the MnO contents were still relatively high compared to the charges containing HCFeMn slag. This shows good accordance with the TGA results in Figure 3, which imply that most of the mass change was due to MnO reduction between 1500 and 1650°C.

The a_{MnO} also represents the reduction of MnO for all charges. Figure 4 compares the a_{MnO} for all charges between 1500 and 1650°C. Note that each point represents an experimental run. The a_{MnO} for all the charges was similar at 1500°C: approximately 0.2 (1550°C for 'Com/HCS'). Only for charges containing HCFeMn slag have the a_{MnO} values dropped down near to zero at 1650°C, which also indicates a higher degree of MnO reduction. This implies that the driving force for MnO reduction ($a_{MnO} - a_{Mn} \approx a_{MnO}$) will have insignificant impact on the reduction rate according to Equations [1] and [2] at the start of reduction Hence it is not the driving force, but the rate constant, that differs more between the reactions occurring with different charges.

The rate constants in this study are expressed as the Arrhenius equation according to Equations [1] and [2]. The Arrhenius plots of MnO and SiO_2 reduction for all charges are described in Figure 5, and the estimated activation energies are shown in Table IV. The Arrhenius plot for MnO reduction shows that charges containing HCFeMn slag have higher rate constants

Table IV

Summary of the estimated activation energies for MnO and SiO_2 reduction between 1500 and 1650°C

Charge	MnO reduction (kJ/mol)	SiO_2 reduction (kJ/mol)
As	250	160
As/HCS	920	870
Com	305	450
Com/HCS	500	790
HCS	780	1130

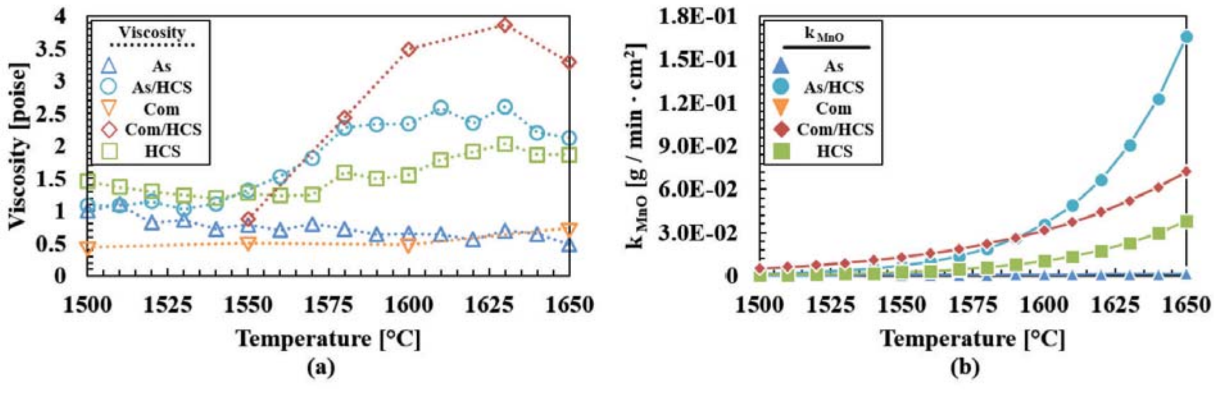

Figure 6—Comparison of (a) slag viscosity and (b) rate constants (MnO reduction) between 1500 and 1650°C

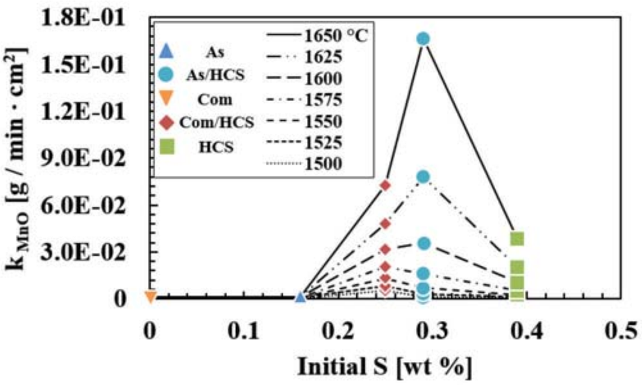

Figure 7 – Comparison of initial amount of sulphur in charge and rate constants (MnO reduction) between 1500 and 1650°C

with increasing temperature. Also, the temperature dependency (activation energy) seems to be similar with different charges types: charges including HCFeMn slag ('As/HCS', 'Com/HCS', and 'HCS') were approximately between 500 and 920 kJ/mol and charges without HCFeMn slag ('As' and 'Com') were between 250 and 300 kJ/mol. The Arrhenius plot for SiO_2 reduction was difficult to estimate due to small amount of Si produced. However, the temperature dependencies for SiO_2 reduction were somewhat similar within the range of experimental conditions.

As the main difference between the different charges is the rate constant, the rate constants for MnO reduction were compared with the viscosity of the slag (Figure 6). If the assumption of chemical reaction being rate-determining is not valid, the viscosity could affect the rate. The viscosities were calculated by using FactSage 7.0 (CRCT and GTT, 2015). No correlation between the viscosity of the slag in the initial phase of the reduction was found at 1500°C, and the rate constant is hence not affected by the viscosity in the slag and probably neither the diffusion, which can be correlated with viscosity.

Sulphur is known to behave as a strong surface-active species for most metals (Stølen and Grande, 2004). The comparison of the initial amount of sulphur in the charge and the rate constants (MnO reduction) between 1500 and 1650°C is shown in Figure 7. Note that the amount of sulphur was calculated from the raw materials (excluding coke). It is seen that the rate constant initially increases with the sulphur content and then decreases again. This is in accordance with previous observations where the sulphur content was studied separately (Kim and Tangstad, 2018a, 2018b, 2018c; Kawamoto, 2016; Larrsen, 2016).

By applying the estimated kinetic parameters in Figure 5, the changing amounts of MnO and SiO_2 in SiMn slags can be described by using the rate models (Equations [1] and [2]). The comparisons between the rate models and the measured amount of MnO and SiO_2 between 1500 and 1650°C are described in Figure 8. Note that the parameters which describe the optimal fit were applied to the rate models (approximately 2% error in the raw materials analyses). The comparison showed that the rate models considered in this study are applicable to describe the amounts of MnO and SiO_2 for SiMn slags. The symbols, which indicate the measured amounts of MnO and SiO_2 from the experiments, show a good match with the calculated amounts (solid and dotted lines) between 1500 and 1650°C. The considered rate models were successfully used to describe the changing amounts of MnO and SiO_2 regardless of the charge type and degree of reduction.

Conclusions

The objective of this study was to estimate the kinetics of MnO and SiO_2 reduction in SiMn slags and to observe the reduction rate between 1500 and 1650°C. The results showed that SiMn charges containing HCFeMn slag as raw material are reduced faster than those without. The measured amount of MnO in slag at 1650°C was low for charges containing HCFeMn slag, and the a_{MnO} showed good accordance: The a_{MnO} was around 0.2 at 1500°C but decreased to near zero at 1650°C. Also, the a_{MnO} at 1500°C was approximately 0.2 for all charges, which implies a low contribution to the driving force for reduction rate. From the kinetic estimations, the activation energies differed for the two types of charge: for MnO reduction, the values for charges containing HCFeMn slag were approximately 500–920 kJ/mol, and for those without, approximately 250–300 kJ/mol. The comparison of slag viscosity with rate constants showed that slag viscosity does not significantly influence the reduction rate of MnO. Instead, small amounts of sulphur impurity in the charge showed significant impact on the reduction rates. At more than 0.15 wt% of initial sulphur, the rate constants increased drastically with increasing temperature. In addition, the

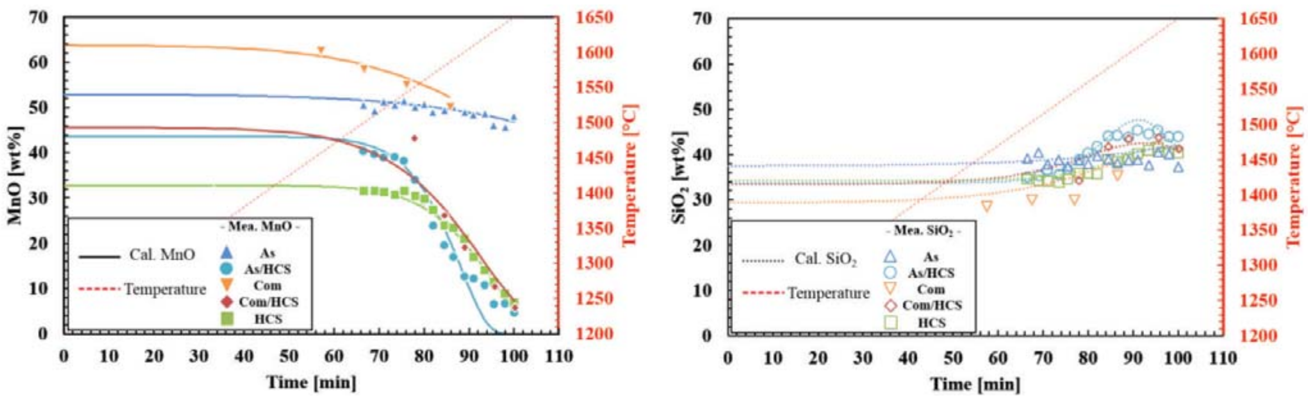

Figure 8 – Comparison of calculated (solid and dotted lines) and measured (symbols) amounts of MnO and SiO_2 in SiMn slags between 1200 and 1650°C

considered rate models for MnO and SiO_2 reduction were able to describe the changing amounts of MnO and SiO_2 in SiMn slags. The results are applicable for estimating the production rate during SiMn smelting.

Acknowledgments

This publication has been partly funded by the SFI Metal Production (Centre for Research-based Innovation, 237738). The authors gratefully acknowledge the financial support from the Research Council of Norway and the partners of the SFI Metal Production.

References

CRCT: Canada, GTT: Germany. FactSage 7.0 http://www.factsage.com

Holtan, J. 2015. Phase composition in Comilog charges during heating and reduction. Internal report: TMT 4500 Materials Technology, Specialization Project, Norwegian University of Science and Technology.

International Manganese Institute. 2014. http://www.manganese.org

Kawamoto, R. 2016. Effect of sulfur addition on reduction mechanism of synthetic ore. Internal report: TMT 4500 Materials Technology, Specialization Project, Norwegian University of Science and Technology.

Kim P., Holtan J., and Tangstad M. 2016. Reduction behavior of Assmang and Comilog ore in the SiMn process. *Proceedings of the 10th International Conference on Molten Slags, Fluxes and Salts (MOLTEN 16),* Seattle, Washington, 22–25 May 2016. Wiley. pp. 1285–1292.

Kim P., Larrsen T., Tangstad M., and Kawamoto R. 2017. Empirical activation energies of MnO and SiO_2 reduction in SiMn slags between 1500 and 1650°C. *Applications of Process Engineering Principles in Materials Processing, Energy and Environmental Technologies.* Wang, S., Free, M., Alam, S., Zhang, M., and Taylor. P. (eds). The Minerals, Metals & Materials Series. Springer. pp. 475–483.

Kim P. and Tangstad M. 2018a. The effect of sulfur content on the reduction rate in SiMn slags. *Metallurgical. Transactions. B* (in press).

Kim P. and Tangstad M. 2018b. The effect of sulfur for MnO and SiO_2 reduction in synthetic SiMn slag. *Metallurgical. Transactions. B* (in press).

Kim P. and Tangstad M. 2018c. Melting behavior of Assmang ore and quartz in the SiMn process. *Metallurgical. Transactions. B* (in press).

Larrsen T. 2016. Reduction of MnO and SiO_2 from Comilog-based charges. Internal report: TMT 4500 Materials Technology, Specialization Project, Norwegian University of Science and Technology (NTNU).

Maroufi S., Ciezki G., Jahanshahi S., Shouyi S., and Ostrovski O. 2015. Dissolution of silica in slag in SiMn production. *Infacon XIV - Proceedings of the Fourteenth International Ferro-Alloys Congress,* Kyiv, Ukraine, 1-4 June 2015. pp. 479–487. https://www.pyrometallurgy.co.za/InfaconXIV/479-Maroufi.pdf

Olsen, H. 2016. A theoretical study on the reaction rates in the SiMn production process. Master's thesis, Department of Materials Science and Engineering, Norwegian University of Science and Technology (NTNU).

Olsen, S.E., Tangstad, M. and Lindstad, T. 2007. Production of manganese ferroalloys. Tapir Academic Press, Trondheim, Norway.

Ostrovski. O., Olsen. S.E., Tangstad. M., and Yastreboff. M. 2002. Kinetic modelling of MnO reduction from manganese ore. *Canadian Metallurgical Quarterly,* vol. 41, no. 3. pp. 309–318.

Outotec. Not dated. HSC Chemistry 7. www.hsc-chemistry.com

Skjervheim, T. 1994. Kinetics and mechanisms for transfer of manganese and silicon from molten oxides to liquid manganese metal. PhD thesis, Department of Metallurgy, Norwegian Institute of Technology (NTNU) .

Stølen, S. and Grande, T. 2004. Chemical thermodynamics of materials. Wiley, Chichester, UK.

Subramanyam, D K., Swansiger, A.E., and Avery, H.S. 1990. Austenitic manganese steels. *ASM Handbook Volume 1, Properties and Selection: Irons, Steels, and High-Performance Alloys.* ASM International. Materials Park, OH.

Tomota, Y., Strum, M., and Morris, Jr. J. 1987. The relationship between toughness and microstructure in Fe-high Mn binary alloys. *Metallurgical Transactions* A, vol. 18A. pp. 1073–1081.

Tranell, G., Gaal, S., Lu, D., Tangstad, M., and Safarian, J. 2007. Reduction kinetics of manganese oxide from HCFeMn slags. *Infacon 11, Proceedings of the Eleventh International Ferro-Alloys Congress.* New Delhi, India, 18-21 February 2007. Indian Ferro Alloy Producers Association. pp. 231–240. https://www.pyrometallurgy.co.za/InfaconXI/231-Tranell.pdf ◆

Erratum - June 2018

It has come to our attention that some text in the Summary and Conclusions and the Acknowledgment in the paper entitled: '**Reduction of Kemi chromite with methane**', by M. Leikola*, P. Taskinen*, and R.H. Eric*†' was omitted. The paper was published in the SAIMM *Journal* vol. 118, no. 6, pp. 575–580.

The complete wording for paragraph 4 should read as follows:

'Metallization was observed to start immediately after the chromite was exposed to CH_4-H_2 mixtures, as chromite reduction to metal was observable after only 10 minutes of reduction time. At temperatures of 1300°C and 1350°C, metallization was completed within the duration of the experiments, as only very small amounts of iron and chromium remained in the unreacted zones. Therefore, reduction of Kemi chromite with a CH_4-H_2 mixture can be regarded as highly efficient compared to reduction with only solid carbon as the reductant. Similar levels of almost complete reduction of chromite spinels by ordinary carbothermic reduction require temperatures over 1500°C. This can be attributed to the high thermodynamic activity of carbon when it is provided by cracking of methane into carbon and hydrogen'.

Acknowledgements

The authors are grateful to Tekes and Finland Academy for providing the part-time Finland Distinguished Professor position to R.H. Eric and funds for this research project. The CMEco project and the Technology Industries of Finland Centennial Foundation are acknowledged for their collaboration and support.

The appropriate correction has been made to the copy of the June 2018 *Journal* on the SAIMM website.